Anilino Radical Complexes of Cobalt(III) and Manganese(IV) and Comparison with Their Phenoxyl Analogues

6 **AUTHORS**, INCLUDING:

Sophie Lecomte
Université Bordeaux 1

78 PUBLICATIONS   **1,125** CITATIONS

Anilino Radical Complexes of Cobalt(III) and Manganese(IV) and Comparison with Their Phenoxyl Analogues

Frank N. Penkert, Thomas Weyhermüller, Eckhard Bill, Peter Hildebrandt, Sophie Lecomte, and Karl Wieghardt*

Contribution from the Max-Planck-Institut für Strahlenchemie, D-45413 Mülheim an der Ruhr, Germany

Received May 12, 2000

Abstract: The pendent arm macrocyclic aniline ligands 1-(2-amino-3,5-di-*tert*-butylbenzyl)-4,7-dimethyl-1,4,7-triazacyclononane, H[L^1], and 1,4,7-tris(2-amino-3,5-di-*tert*-butylbenzyl)-1,4,7-triazacyclononane, H$_3$[L^2], have been synthesized. The reaction of these ligands in methanol (1:1) and/or ethanol with Co^{II}(ClO$_4$)$_2$·6H$_2$O and potassium di-*tert*-butylacetylacetonate (1:1) or Mn^{II}(acetate)$_2$·4H$_2$O in the presence of air produced the anilido complexes [Co^{III}(L^1)(Bu$_2$acac)](ClO$_4$) (**1**) and [Mn^{IV}(L^2)]X (X = ClO$_4$ (**2**), BPh$_4$ (**2′**)), respectively. The reaction of H$_3$[L^2] and CuCl$_2$·2H$_2$O in ethanol produced upon addition of NaClO$_4$ blue crystals of [Cu^{II}(H$_3$L^2)Cl]-(ClO$_4$) (**3**) containing two coordinated and one uncoordinated aniline pendent arm. Complexes **1**, **2**, and **3** have been structurally characterized by X-ray crystallography. Electrochemically, **1** is reversibly oxidized with formation of the paramagnetic anilino radical species [Co^{III}(L$^{1•}$)(Bu$_2$acac)]$^{2+}$ ($S = \frac{1}{2}$) whereas the cyclic voltammogram of **2** displays three ligand-centered one-electron-transfer oxidation waves where complexes [Mn^{IV}(L$^{2•}$)]$^{2+}$, [Mn^{IV}(L$^{2••}$)]$^{3+}$, and [Mn^{IV}(L$^{2•••}$)]$^{4+}$ containing one, two, and three coordinated anilino radicals are formed successively. These anilino radical species have been characterized by UV−vis, X-band EPR, and resonance Raman spectroscopy. The characteristic spectroscopic features of coordinated anilino radicals have been elucidated. In the Mn^{IV} radical species strong intramolecular exchange coupling between the metal ion (t$_{2g}^3$ configuration, $S = 3/2$) and one, two, or three anilino radicals ($S_{rad} = 1/2$) produces the ground states $S_t = 1$, $S_t = 1/2$, and $S_t = 0$ in the di-, tri-, and tetracation of the parent complex **2**, respectively.

Introduction

Tyrosyl radicals coordinated or uncoordinated to a transition metal ion have been identified in a steadily increasing number of metalloproteins as essential cofactors.[1] Consequently, inorganic chemists have studied in depth the coordination chemistry of (phenoxyl)metal complexes and identified spectroscopic markers for this class of radical compounds.[2] The most effective spectroscopic tools in this respect proved to be resonance Raman[3] and EPR spectroscopy[4] in conjunction with X-ray absorption spectroscopy (XAS).[5]

The coordination chemistry of the isoelectronic anilino radical has in the past received much less attention. While the parent

compounds, namely, the anilino radical, Ph−N̊H, and its protonated radical cation, [Ph−N̊H$_2$]$^+$, have been generated by pulse radiolysis and studied by UV/vis,[6] EPR,[7] and RR spectroscopy[8] in aqueous solution as well as by computational methods,[9] their coordination chemistry with transition metal ions has been plagued by the inherent ambiguity of assigning the correct oxidation level to both the ligand (aminyl vs amide) and the metal ion. (The nomenclature used in the literature is slightly confusing. In coordination compounds we designate a coordinated Ph−NH$_2$ moiety as aniline (amine) and its monoanion Ph−NH$^-$ as anilido whereas the coordinated neutral radical Ph−N̊H is designated as anilino following organic nomenclature.) The question arises whether the structures A and B
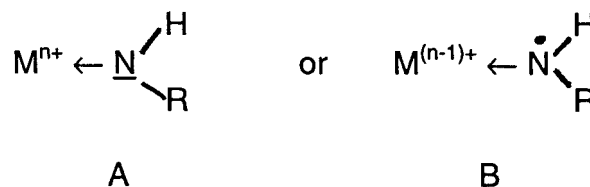
represent two resonance structures of a single electronic ground state or, alternatively, are they two different species (redox

(1) (a) Chaudhuri, P.; Wieghardt, K. *Progr. Inorg. Chem.,* in press. (b) Stubbe, J. A. *Biochemistry* **1988,** *27,* 3893. (c) Stubbe, J. A. *Annu. Rev. Biochem.* **1989,** *58,* 257. (d) *Metal Ions in Biological Systems;* Sigel, H., Sigel, A., Eds.; Marcel Dekker, Inc.: New York, 1994; Vol. 30.
(2) (a) Adam, B.; Bill, E.; Bothe, E.; Goerdt, B.; Haselhorst, G.; Hildenbrand, K.; Sokolowski, A.; Steenken, S.; Weyhermüller, T.; Wieghardt, K. *Chem. Eur. J.* **1997,** *3,* 308. (b) Müller, J.; Kikuchi, A.; Bill, E.; Weyhermüller, T.; Hildebrandt, P.; Ould-Moussa, L.; Wieghardt, K. *Inorg. Chim. Acta* **2000,** *297,* 265. (c) Sokolowski, A.; Müller, J.; Weyhermüller, T.; Schnepf, R.; Hildebrandt, P.; Hildenbrand, K.; Bothe, E.; Wieghardt, K. *J. Am. Chem. Soc.* **1997,** *119,* 8889. (d) Sokolowski, A.; Leutbecher, H.; Weyhermüller, T.; Schnepf, R.; Bothe, E.; Bill, E.; Hildebrandt, P.; Wieghardt, K. *J. Biol. Inorg. Chem.* **1997,** *2,* 444. (e) Sokolowski, A.; Adam, B.; Weyhermüller, T.; Kikuchi, A.; Hildenbrand, K.; Schnepf, R.; Hildebrandt, P.; Bill, E.; Wieghardt, K. *Inorg. Chem.* **1997,** *36,* 3702.
(3) Schnepf, R.; Sokolowski, A.; Müller, J.; Bachler, V.; Wieghardt, K.; Hildebrandt, P. *J. Am. Chem. Soc.* **1998,** *120,* 2352.
(4) Babcock, G. T.; El-Deeb, M. K.; Sandusky, P. O.; Whittaker, M. M.; Whittaker, J. W. *J. Am. Chem. Soc.* **1992,** *114,* 3727.
(5) (a) Clark, K.; Penner-Hahn, J. E.; Whittaker, M. M.; Whittaker, J. W. *J. Am. Chem. Soc.* **1990,** *112,* 6433. (b) Clark, K.; Penner-Hahn, J. E.; Whittaker, M. M.; Whittaker, J. W. *Biochemistry* **1994,** *33,* 12553. (c) Knowles, P. F.; Brown, R. D., III; Koenig, S. H.; Wang, S.; Scott, R. A.; McGuirl, M. A.; Brown, D. E.; Dooley, D. M. *Inorg. Chem.* **1995,** *34,* 3895. (d) Wang, Y.; DuBois, J. L.; Hedman, B.; Hodgson, K. O.; Stack, T. D. P. *Science* **1998,** *279,* 537.

(6) (a) Qin, L.; Tripathi, G. N. R.; Schuler, R. H. *Z. Naturforsch.* **1985,** *40a,* 1026. (b) Wigger, A.; Grünbein, A.; Henglein, A.; Land, E. J. *Z. Naturforsch.* **1969,** *24b,* 1262. (c) Christensen, H. *Int. J. Radiat. Phys. Chem.* **1972,** *4,* 311.
(7) (a) Neta, P.; Fessenden, R. W. *J. Chem. Phys.* **1974,** *78,* 523. (b) Land, E. J.; Porter, G. *J. Chem. Soc.* **1961,** 3540. (c) Atherton, N. M.; Land, E. J.; Porter, G. *Trans. Faraday Soc.* **1963,** *59,* 818.
(8) (a) Tripathi, G. N. R.; Schuler, R. H. *J. Chem. Phys.* **1987,** *86,* 3795. (b) Tripathi, G. N. R.; Schuler, R. H. *Chem. Phys. Lett.* **1984,** *110,* 542.
(9) Adamo, C.; Subra, R.; DiMatteo, A.; Barone, V. *J. Chem. Phys.* **1998,** *109,* 10244.

Scheme 1. Complexes from Reference 10

Scheme 2. Ligands and Complexes
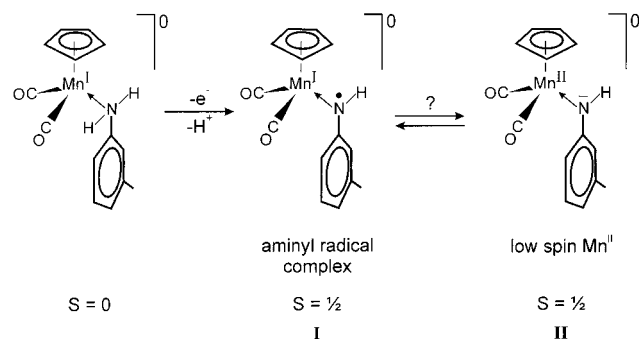
isomers) with two distinctly different ground states. For example, in 1982 Sellmann et al. reported a series of organometallic compounds which they described as (aminyl)manganese(I) complexes (Scheme 1).[10] Kaim et al.[11] in 1985 showed that the spectroscopic data (EPR, UV/vis) of these compounds are probably more in agreement with the formulation as (amido)-manganese(II) species, where the manganese(II) has a low-spin configuration ($S = 1/2$).

Thus the present paper represents the first report on transition metal ion compounds that unambiguously contain coordinated anilino radicals. The parent anilino radical is a very reactive intermediate that undergoes rapid radical combination reactions. The radical cation, $Ph-\dot{N}H_2^+$, combines by way of C−C or C−N coupling whereas the neutral radical, $Ph-\dot{N}H$, undergoes C−N and N−N couplings.[12] To suppress these reactions and thereby increase the lifetime of the radicals, the ortho and para positions of the aniline moiety must be protected by bulky substituents. The 2,4,6-tri-*tert*-butylanilino radical is a stable species in solution.[7b]

In this work we have synthesized the ligands 1-(2-amino-3,5-di-*tert*-butylbenzyl)-4,7-dimethyl-1,4,7-triazacyclononane, H[L^1], and 1,4,7-tris(2-amino-3,5-di-*tert*-butylbenzyl)-1,4,7-triazacyclononane, H$_3$[L^2], and prepared the precursor complexes [(L^1)Co^{III}(Bu$_2$acac)](ClO$_4$) (**1**), [(L^2)Mn^{IV}](ClO$_4$) (**2**), and [(H$_3$L^2)-CuCl]ClO$_4$ (**3**) as shown in Scheme 2. The corresponding phenolato complexes [(L^{Pr})Co^{III}(acac)]ClO$_4$[2e] and [(L^{Bu})Mn^{IV}]-PF$_6$[2a] have been described previously. It has been shown that each of the coordinated phenolato groups can be converted via a reversible one-electron oxidation to a coordinated phenoxyl ligand. H[L^{Pr}] represents the ligand 1,4-diisopropyl-7-(3,5-di-*tert*-butyl-2-hydroxybenzyl)-1,4,7-triazacyclononane, which was originally prepared by Tolman et al.,[13] and H$_3$[L^{Bu}] is 1,4,7-tris(3,5-di-*tert*-butyl-2-hydroxybenzyl)-1,4,7-triazacyclono-nane.[2a] We will compare the spectroscopic features of coordinated anilino ligands with those of the corresponding coordinated phenoxyls.

The first indication that anilino radical complexes might be stable was obtained in 1995 in our laboratory when we reported that the tris(anilido)manganese(IV) complex [Mn^{IV}(L^a)]BPh$_4$,[14] where H$_3$[L^a] is 1,4,7-tris(*o*-aminobenzyl)-1,4,7-triazacyclono-nane,[15] which is unprotected at the ortho and para positions, displays three irreversible oxidation waves at quite positive
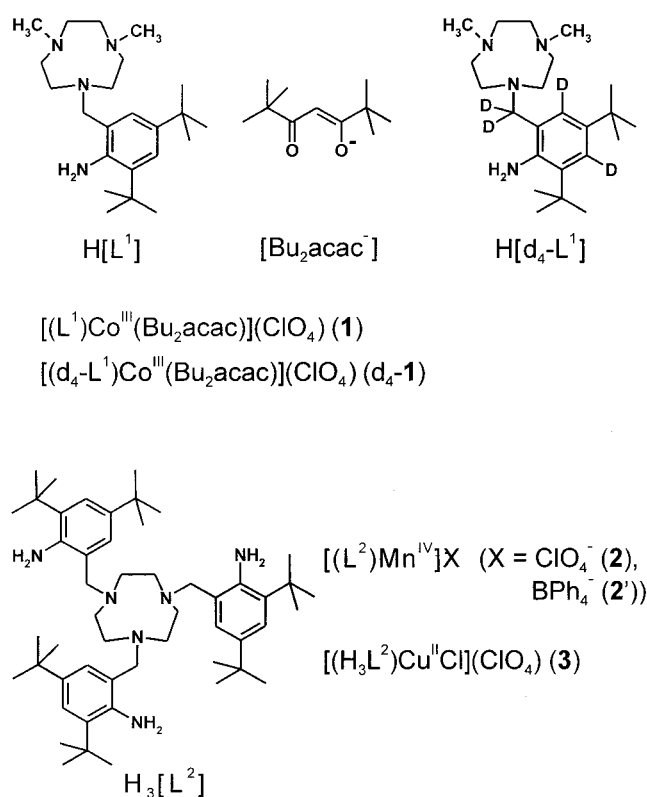
potentials in the cyclic voltammogram. At that time we speculated that these might be metal-centered processes involving Mn^V and Mn^{VI}, but it was noted that they might also be ligand-centered processes. If the latter is the case, these oxidations are irreversible because the generated unprotected anilino radicals undergo rapid combination reactions as described above for the parent anilino radical.

Experimental Section

Preparation of Ligands. 3,5-Di-*tert*-butyltoluene[16] and 3,5-di-*tert*-butyl-2-nitrotoluene[17] were synthesized according to published procedures.

3,5-Di-*tert*-butyl-2-nitrobenzylbromide. A solution of 3,5-di-*tert*-butyl-2-nitrotoluene (24.9 g; 0.10 mol) and *N*-bromosuccinimide (NBS) (17.8 g; 0.1 mol) in CCl$_4$ (250 mL) was heated to reflux, and azobisisobutyronitrile was added as a radical starter. The solution was stirred without heating but with irradiation (white light) until all of the generated succinimide floated on top of the solution. To the filtered solution was added a saturated aqueous NaHCO$_3$ solution with stirring. The phases were separated, and the organic phase was dried over MgSO$_4$. After removal of the solvent under reduced pressure the residue was recrystallized from methanol and then from *n*-pentane. Yield: 23.0 g (70%). EI mass spectrum: 329 *m/z* {M$^+$}, mp 77 °C. ^{1}H NMR-(CDCl$_3$): $\delta = 1.31$ (s, 9H, t-Bu), 1.37 (s, 9H, t-Bu), 4.32 (s, 2H, CH$_2$), 7.35 (s, 1H, aromatic proton), 7.51 (s, 1H, aromatic proton). ^{13}C NMR-(CDCl$_3$): $\delta = 27.4$ (CH$_2$), 30.9 (t-Bu, CH$_3$), 31.1 (t-Bu, CH$_3$), 35.1 (t-Bu, C^4), 36.1 (t-Bu, C^4), 126.1 (Ph−H), 126.3 (Ph−H), 129.0, 140.5, 153.1.

(10) (a) Sellmann, D.; Müller, J.; Hofmann, P. *Angew. Chem.* **1982**, *94*, 708; *Angew. Chem., Int. Ed. Engl.* **1982**, *21*, 691. (b) Sellmann, D.; Müller, J. *J. Organomet. Chem.* **1985**, *281*, 249.

(11) (a) Gross, R.; Kaim, W. *Angew. Chem.* **1985**, *97*, 869; *Angew. Chem., Int. Ed. Engl.* **1985**, *24*, 856. (b) Gross, R.; Kaim, W. *Inorg. Chem.* **1987**, *26*, 3596.

(12) Merényi, G.; Lind, J. In *N-centered Radicals*; Alfassi, Z. B., Ed.; John Wiley and Sons Ltd.: New York, 1998; p 599.

(13) Halfen, J. A.; Young, V. G.; Tolman, W. B. *Angew. Chem., Int. Ed. Engl.* **1996**, *35*, 1687.

(14) Schlager, O.; Wieghardt, K.; Nuber, B. *Inorg. Chem.* **1995**, *34*, 6456.

(15) (a) Schlager, O.; Wieghardt, K.; Nuber, B. *Inorg. Chem.* **1995**, *34*, 6449. (b) Schlager, O.; Wieghardt, K.; Grondey, H.; Rufinska, A.; Nuber, B. *Inorg. Chem.* **1995**, *34*, 6440.

(16) Risch, N.; Meyer-Roscher, B.; Langhals, M. *Z. Naturforsch.* **1994**, *49*, 141.

(17) (a) Beets, M. G. J.; Meerburg, W.; von Essen, H. *Recl. Trav. Chim. Pays-Bas* **1959**, *78*, 570. (b) Geuze, J.; Ruinard, C.; Soeterbraenk, J.; Verkade, P. E.; Wepster, B. M. *Recl. Trav. Chim. Pays-Bas* **1956**, *75*, 301. (c) Myhre, P. C.; Beng, M.; James, L. L. *J. Am. Chem. Soc.* **1968**, *90*, 2105. (d) Crivello, J. V. *J. Org. Chem.* **1981**, *46*, 3056.

1-(3,5-Di-*tert*-butyl-2-nitrobenzyl)-4,7-dimethyl-1,4,7-triazacyclononane. A suspension of 1,4-dimethyl-1,4,7-triazacyclononane[18] (0.79 g; 5.0 mmol), 3,5-di-*tert*-butyl-2-nitrobenzylbromide (2.46 g; 7.5 mmol), and solid KOH (1.7 g; 30 mmol) in toluene (50 mL) was heated to 80 °C with stirring for 16 h. The solid material was filtered off and discarded, and the solution was dried over $MgSO_4$. After removal of the solvent by evaporation under reduced pressure, the residue was dissolved in methanol (20 mL) to which concentrated HCl (20 mL) was added. More methanol was added until a clear solution was obtained, which was extracted with diethyl ether (5 × 20 mL). The solvent was removed by rotary evaporation from the acidic methanol solution, and the residue was redissolved in methanol (20 mL) to which Na[OCH_3] was added (neutralization). After addition of aqueous 5 M KOH (50 mL), the solution was extracted with a large amount of *n*-pentane. The solution was dried over $MgSO_4$, and the solvent was removed. An oily product was obtained. Yield: 1.90 g (94%). EI mass spectrum: $m/z = 404$ (M^+). ^{1}H NMR($CDCl_3$): $\delta = 1.31$ (s, 9H, t-Bu), 1.36 (s, 9H, t-Bu), 2.33 (s, 6H, CH_3), 2.66 (m, 8H, CH_2–CH_2), 2.77 (s, 4H, CH_2–CH_2), 3.50 (s, 2H, CH_2), 7.40 (d, 1H, $J = 2.0$ Hz, aromatic H), 7.53 (d, 1H, $J = 2.0$ Hz, aromatic H). ^{13}C NMR($CDCl_3$): $\delta = 31.0$ (t-Bu, CH_3), 31.2 (t-Bu, CH_3), 35.0 (t-Bu, C^4), 35.9 (t-Bu, C^4), 46.6 (CH_3), 56.5, 56.8, 57.0 (CH_2–CH_2), 58.7 (CH_2), 123.7, 125.7, 131.4, 139.5, 148.2, 151.9 (phenyl ring).

1-(2-Amino-3,5-di-*tert*-butylbenzyl)-4,7-dimethyl-1,4,7-triazacyclononane (H[L^1]). The above nitro compound (1.9 g; 4.7 mmol) was dissolved in dry tetrahydrofurane (THF) (65 mL) to which solid Li-[AlH_4] (1.8 g; 47 mmol) was carefully added with stirring. The mixture was slowly heated to 80 °C and stirred at this temperature for 16 h. A saturated aqueous solution (100 mL) of Na_2[S_2O_4] was added. After 20 min the solid was filtered off and washed with water and diethyl ether. From the filtrate the product was extracted with diethyl ether, and KOH was added to the aqueous phase (pH ~ 14) and again extracted with diethyl ether. The combined ether phase was dried over $MgSO_4$ and the solvent removed under reduced pressure. The following workup was done as described above: the residue was redissolved in CH_3OH/HCl and washed with $CHCl_3$ (5 × 20 mL), the solvent was removed, the residue was dissolved in H_2O and NaOH was added, and extraction was carried out with *n*-pentane. The product was obtained as a yellow oil. Yield: 1.37 g (78%). EI mass spectrum: $m/z = 374$ (M^+). ^{1}H NMR($CDCl_3$): $\delta = 1.25$ (s, 9H, t-Bu), 1.42 (s, 9H, t-Bu), 2.31 (s, 6H, CH_3), 2.60−2.75 (m, 12H, CH_2–CH_2), 3.60 (s, 2H, CH_2), 5.04 (broad s, 2H, NH_2), 6.86 (d, 1H, $J = 2.3$ Hz, aromatic H), 7.18 (d, 1H, $J = 2.3$ Hz, aromatic H). ^{13}C NMR($CDCl_3$): $\delta = 30.0$, 31.7 (t-Bu, CH_3), 34.0, 34.4 (t-Bu, C^4), 46.6 (CH_3), 55.1, 57.7, 57.8 (CH_2–CH_2), 63.5 (CH_2), 122.4 (Ph−H), 124.1, 125.7 (Ph−H), 130.0, 132.6, 139.0 (aromatic C).

1,4,7-Tris(3,5-di-*tert*-butyl-2-nitrobenzyl)-1,4,7-triazacyclononane. A suspension of 1,4,7-triazacyclononane (2.65 g; 20 mmol), 3,5-di-*tert*-butyl-2-nitrobenzylbromide (23.0 g; 70 mmol), and solid KOH (9.0 g; 160 mmol) in toluene (300 mL) was heated at 80 °C for 16 h with stirring. After filtration the solution was dried over Na_2SO_4. Removal of the solvent by rotary evaporation produced a pale yellow solid, which was recrystallized from methanol. Yield: 11.3 g (65%). EI mass spectrum: $m/z = 870$ (M^+), mp 134 °C. ^{1}H NMR($CDCl_3$): $\delta = 1.30$ (s, 27H, t-Bu), 1.35 (s, 27H, t-Bu), 2.70 (broad s, 12H, CH_2-CH_2), 3.48 (s, 6H, CH_2), 7.40 (d, 3H, $J = 2.0$ Hz, Ph−H), 7.51 (d, 3H, $J = 2.0$ Hz, Ph−H). ^{13}C NMR($CDCl_3$): $\delta = 31.0$ (t-Bu, CH_3), 31.2 (t-Bu, CH_3), 35.0 (t-Bu, C^4), 35.9 (t-Bu, C^4), 55.6 (CH_2CH_2), 58.6 (CH_2), 123.8, 125.8 (Ph−H), 131.3, 139.5, 148.2, 152.0 (Ph).

1,4,7-Tris(2-amino-3,5-di-*tert*-butylbenzyl)-1,4,7-triazacyclononane, H$_3$[L^2]. To the solution of the above tris(nitro) derivative (8.71 g; 10 mmol) in THF (150 mL) was added Li[AlH_4] (3.8 g; 0.1 mmol) with stirring. The mixture was slowly heated to 80 °C and stirred at this temperature for 16 h. The workup was performed as follows: To the reaction mixture was added a saturated aqueous solution of Na_2-[S_2O_4] (100 mL). After filtration the product was extracted from the aqueous phase with diethyl ether. Removal of the solvent produced a pale yellow residue, which was redissolved in $CHCl_3$. After filtration

and evaporation of the solvent the solid product was obtained. Yield: 6.6 g (85%). EI mass spectrum: $m/z = 780$ (M^+), mp 212 °C. ^{1}H NMR-($CDCl_3$): 1.23 (s, 27H, t-Bu), 1.43 (s, 27H, *t*-Bu), 2.58 (broad s, 12H, CH_2−CH_2), 3.52 (s, 6H, CH_2), 5.04 (broad s, 6H, NH_2), 6.79 (d, 3H, $J = 2.1$ Hz, Ph−H), 7.20 (d, 3H, $J = 2.1$ Hz, Ph−H). ^{13}C NMR-($CDCl_3$): $\delta = 30.0$ (t-Bu, CH_3), 31.7 (t-Bu, CH_3), 34.0 (t-Bu, C^4), 34.4 (t-Bu, C^4), 56.3 (CH_2−CH_2), 64.1 (CH_2), 122.6, 123.7 (Ph−H), 125.8, 132.7, 139.2, 142.6 (Ph).

Preparation of Complexes. [Co^{III}(L^1)(Bu_2acac)](ClO_4) (1). To a solution of the ligand H[L^1] (0.22 g; 0.6 mmol) in methanol was added Co(ClO_4)$_2$·6H_2O (0.16 g; 0.6 mmol) with stirring. The solution was heated to reflux under argon for 1 h after which time potassium di-*tert*-butylacetylacetonate (0.13 g; 0.6 mmol) was added. Stirring in the presence of air was continued for 2 h. After filtration a green precipitate formed from the solution, which was collected by filtration. Yield: 52.5 mg (12%). EI mass spectrum: $m/z = 714$ ([Co(L^1)(Bu_2acac)]$^+$). ^{1}H NMR($CDCl_3$): $\delta = 0.68$ (s, 9H, t-Bu), 1.20 (s, 18H, t-Bu), 1.43 (s, 9H, t-Bu), 2.24 (s, 3H, CH_3), 2.25 (s, 3H, CH_3), 2.47−3.80 (m, 12H, CH_2−CH_2), 2.67 (d, 1H, $J = 15.1$ Hz, CH_2), 4.05 (d, 1H, $J = 15.1$ Hz, CH_2), 5.78 (s, 1H, CH), 6.68 (s, 1H, Ph−H), 7.00 (s, 1H, Ph−H). ^{13}C NMR($CDCl_3$): $\delta = 27.7$, 28.6, 31.1, 31.5 (t-Bu, CH_3), 33.9, 35.4, 40.7, 41.0 (t-Bu, C^4), 47.0, 47.6 (CH_3), 55.8, 56.8, 57.5, 58.9, 59.0, 60.8 (CH_2–CH_2), 63.3 (CH_2), 91.9 (CH), 117.1, 123.0, 123.5, 135.8, 137.7, 148.3 (Ph−H), 198.5, 200.2 (CO). Anal. Calcd for $C_{34}H_{60}ClCoN_4O_6$: C, 57.09; H, 8.45; N, 7.83. Found: C, 56.63; H, 8.65; N, 7.35.

[Mn^{IV}(L^2)]X (X = ClO_4 (2), BPh_4·1toluene (2′)). A solution of the ligand H_3[L^2] (0.39 g; 0.5 mmol) and Mn^{II}(acetate)$_2$·4H_2O (0.13 g; 0.5 mmol) in ethanol (25 mL) was heated to reflux with stirring for 2 h under an argon atmosphere. To the cooled solution were added a few drops of triethylamine, and stirring was continued for a few hours in the presence of air whereupon a color change from green to deep blue was observed. To this solution $NaClO_4$ (1.15 g) dissolved in ethanol (50 mL) or, alternatively, Na[BPh_4] (0.34 g; 1 mmol) dissolved in ethanol (50 mL) was added, which initiated the slow precipitation of deep-blue microcrystals of 2 and 2′ in 8 and 22% yield, respectively. Single crystals of 2′ suitable for X-ray crystallography were obtained by slow recrystallization of 2′ from a methanol/toluene mixture (1:1). ESI mass spectrum (pos. ion): $m/z = 832$ ([Mn(L^2)]$^+$). Anal. Calcd for 2′, $C_{82}H_{109}BMnN_6$: C, 79.14; H, 8.83; N, 6.75. Found: C, 78.92; H, 9.03; N, 6.86.

[Cu^{II}(H_3L^2)Cl](ClO_4)·CH_3OH·1.5H_2O (3). A solution of the ligand H_3[L^2] (0.78 g; 1.0 mmol) and $CuCl_2$·2H_2O (0.17 g; 1.0 mmol) in ethanol (25 mL) was stirred at ambient temperature for 15 min after which time a solution of $NaClO_4$ (0.70 g) in ethanol (25 mL) was added. Water (100 mL) was added with stirring, which initiated the precipitation of blue microcrystalline 3. This material was recrystallized from an aqueous methanol solution. Yield: 0.30 g (31%). ESI mass spectrum (pos. ion): $m/z = 880$ ([Cu(H_3L^2)Cl]$^+$). Anal. Calcd for $C_{52}H_{91}Cl_2$-$CuN_6O_{6.5}$: C, 60.13; H, 8.83; N, 8.09. Found: C, 59.76; H, 8.74; N, 8.18.

Crystal Structure Determinations. Green single crystals of **1,** and **3**·MeOH·1.5 H_2O and a blue specimen of **2′**·toluene, were picked up from the mother liquor with a glass fiber and immediately mounted on a Siemens SMART CCD-detector diffractometer equipped with a cryogenic nitrogen cold stream to prevent loss of solvent. Graphite monochromated Mo Kα radiation ($\lambda = 0.71073$ Å) was used. Crystallographic data of the compounds are listed in Table 1. Cell constants for **1**, **2′**, and **3** were obtained from a least-squares fit of the setting angles of 6909, 2856, and 7334 reflections, respectively. Intensity data were collected at −173(2) °C by a hemisphere run taking frames at 0.30° in ω. Data were corrected for Lorentz and polarization effects, and a semiempirical absorption correction for **1** and **3** was carried out using the program SADABS.[19] The Siemens ShelXTL[20] software package was used for solution, refinement, and artwork of the structures. The structures were solved and refined by direct methods and difference Fourier techniques. Neutral atom scattering factors of the software package were used. All non-hydrogen atoms of **1** and **3** were refined anisotropically, except those of disordered anions and solvent molecules,

(18) Alder, R. W.; Mowlam, R. W.; Vachon, D. J.; Weisman, G. R. *J. Chem. Soc., Chem. Commun.* **1992**, 507.

(19) SADABS; Sheldrick, G. M., Universität Göttingen, 1994.
(20) ShelXTL V.5; Siemens Analytical X-ray Instruments, Inc. 1994.

Table 1.   Crystallographic Data for **1,2′**·Toluene, and **3**·MeOH·1.5 H$_2$O

	1	**2′**·toluene	**3**·MeOH·1.5H$_2$O
chem formula	C$_{34}$H$_{60}$ClCoN$_4$O$_6$	C$_{82}$H$_{109}$BMnN$_6$	C$_{52}$H$_{91}$Cl$_2$CuN$_6$O$_{6.5}$
fw	715.24	1244.50	1038.75
space group	$R\bar{3}$	$P2_1/c$	$P\bar{1}$
a, Å	31.994(5)	21.101(4)	13.814(3)
b, Å	31.994(5)	19.209(4)	13.869(3)
c, Å	18.828(3)	18.070(4)	18.171(4)
α, deg	90	90	81.48(3)
β, deg	90	98.14(3)	69.13(3)
γ, deg	120	90	61.20(3)
V, Å^3	16 691(4)	7251(3)	2849.4(11)
Z	18	4	2
T, K	100(2)	100(2)	100(2)
ρ calcd, g cm^3	1.281	1.140	1.211
μ(Mo Kα), cm^{-1}	5.81	2.29	5.28
refl. collected	35 110	19 703	22 724
unique refl./[$I > 2\sigma(I)$]	4569/3095	6354/3159	8981/6612
no. parameters	444	354	671
$2\theta_{max}$, deg	45.0	40.0	50.0
R1^a [$I > 2\sigma(I)$]	0.0731	0.1013	0.0689
wR2^b[$I > 2\sigma(I)$]	0.1637	0.2192	0.1566
goodness of fit (F^2)	1.064	0.955	1.040

^{a} R1 = $\Sigma||F_o| - |F_c||/\Sigma|F_o|$. ^{b} wR2 = $[\Sigma[w(F_o{}^2 - F_c{}^2)^2]/\Sigma[w(F_o{}^2)^2]]^{1/2}$, where $w = 1/\sigma^2(F_o{}^2) + (aP)^2 + bP$, $P = (F_o{}^2 + 2F_c{}^2)/3$.

which were isotropically refined. Diffraction data of **2′** allowed anisotropic refinement of the manganese atom only, since the number of observed reflections was low. Hydrogen atoms were placed at calculated positions and refined as riding atoms with isotropic displacement parameters. The perchlorate anion and solvent molecules in **3** were found to be disordered. A split model with occupancy factors of 0.7 and 0.3 was used to account for the disorder of the anion, but only two of four "oxygen positions" of the minor part could be resolved. Occupancy factors of 0.5 were assigned to two potential methanol molecules and a water molecule of crystallization. Disorder of the perchlorate anion in crystals of **1** was treated by a split model with occupancy factors of 2/3 and 1/3. A residual electron density peak of 2.04 e/Å^3 remained in a potential solvent area of about 130 Å^3, but refinement of a water or methanol molecule did not fit well.

Physical Measurements. Electronic spectra were recorded on a Hewlett-Packard HP 8452A diode array spectrophotometer (range 200–800 nm). X-band EPR spectra of frozen solutions were measured on a Bruker ESP 300E spectrometer, equipped with an Oxford Instruments ESR 910 helium-flow cryostat with an ITC 503 temperature controller. Temperature stability was 0.2 K, and the temperature gradient across the sample was estimated to be less than 0.5 K. X-band EPR spectra at room temperature were measured on a modified Varian EPR spectrometer (Varian E-9X). The data were digitized by means of the data station Stelar DS-EPR (Stelar Inc., Male, Italy). We thank Dr. F. Neese (Abteilung Biologie der Universität Konstanz, Germany) for a copy of his EPR simulation program (version 1.0, 1994) which we used for simulations of $S = 1/2$ spectra measured in fluid solution. High-spin spectra measured in frozen solution were simulated by using the ESIM program package^{21a} S22, S22–I32, S32 fit routines. This program is based on the IRON″ HS routine.^{21b} The ESIM routines allow automatic optimizations of all parameters via a SIMPLEX routine.^{21c} NMR spectra were recorded on Bruker Instruments (ARX 250, DRX 400, and DRX 500). Chemical shifts are referenced vs TMS by using the signals of nondeuterated solvents as internal standards. Cyclic voltammograms, square-wave voltammograms, and coulometric experiments were performed on EG&G equipment (potentiostat/galvanostat model 273A) on Ar flushed CH$_2$Cl$_2$ solutions of samples containing 0.10 M [N(*n*-Bu)$_4$]PF$_6$ as supporting electrolyte under an Ar atmosphere. Potentials were referenced vs Ag/0.10 M AgNO$_3$/CH$_3$-CN electrode; ferrocene was added as internal standard. Resonance Raman spectra were recorded with a U 1000 spectrograph (1200 nm

(21) (a) Bill, E. Unpublished program package ESIM. (b) Gaffney, E. J.; Silverstone, J. In *Biological Magnetic Resonance;* Berliner, L. J., Reuben, J., Eds.; Plenum: New York, 1993; Vol. 13: *EMR of Paramagnetic Molecules.* (c) Press, W. H.; Flannery, B. P.; Tukolsky, S. A.; Vutterly, W. T. *Numerical Recipes*; Cambridge University Press: Cambridge, 1990.

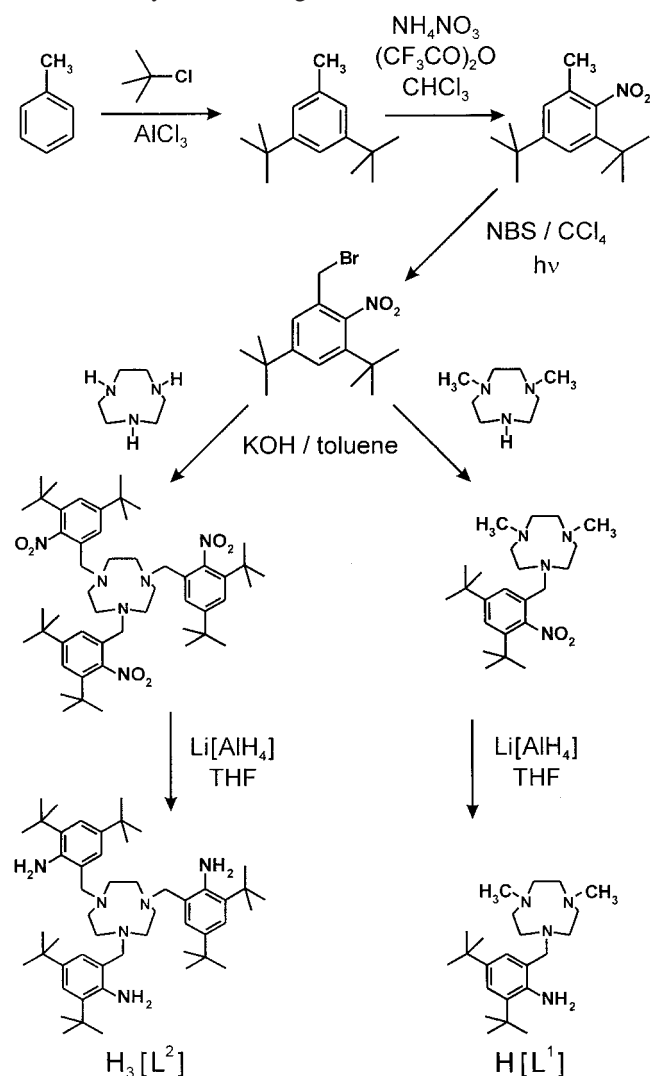halographic gratings) equipped with a liquid nitrogen cooled CCD detector (Jobin Yvon, Spex 2). The 514 nm line output of an Ar ion laser (Innova 400) served as the excitation source. Samples of approximate optical density of 1.5 at the excitation wavelength were placed in a rotating quartz cell. Contributions of the solvent and supporting electrolyte to the spectra were subtracted.

Results

Syntheses. The ligands 1-(2-amino-3,5-di-*tert*-butylbenzyl)-4,7-dimethyl-1,4,7-triazacyclononane, H[L^1], and 1,4,7-tris(2-amino-3,5-di-*tert*-butylbenzyl)-1,4,7-triazacyclononane, H$_3$[L^2], have been prepared by the reaction of di-3,5-*tert*-butyl-2-nitrobenzylbromide with either 1,4-dimethyl-1,4,7-triazacyclononane (1:1) or 1,4,7-triazacyclononane (3:1) in toluene over KOH (Scheme 3). The resulting nitro compounds were reduced to the final amino derivatives with Li[AlH$_4$] in tetrahydrofurane.

A methanol solution of H[L^1] and [Co(H$_2$O)$_6$](ClO$_4$)$_2$ (1:1) was heated to reflux under an argon atmosphere. Potassium di-*tert*-butylacetylacetonate was added, and the resulting solution was stirred in the presence of air. From this solution green microcrystals of diamagnetic [(L^1)Co^{III}(Bu$_2$acac)](ClO$_4$) (**1**) were obtained in ~15% yield.

The reaction of H$_3$[L^2] and Mn^{II}(acetate)$_2$·4H$_2$O and a few drops of NEt$_3$ in ethanol in the presence of air produced a deep blue solution from which the deep-blue salts [Mn^{IV}(L^2)]X$_2$ (X = ClO$_4$ (**2**), BPh$_4$ (**2′**)) were obtained in 20% yield upon addition of NaClO$_4$ or Na[BPh$_4$].

The reaction of H$_3$[L^2] with Cu^{II}Cl$_2$·2H$_2$O in ethanol yields upon addition of an aqueous solution of NaClO$_4$ blue crystals of [(H$_3$L^2)Cu^{II}Cl](ClO$_4$) (**3**).

Crystal Structures. The crystal structures of complexes **1**, **2′**, and **3** have been determined by single-crystal X-ray crystallography at 100(2) K. Selected bond distances and angles are summarized in Table 2; Figure 1 displays the structures of the monocations in crystals of 1 (top), 2 (middle), and 3 (bottom), respectively.

In crystals of **1** a low-spin cobalt(III) ion is octahedrally coordinated to a tetradentate anilido (L^1)$^{1-}$ and a bidentate di-*tert*-butylacetonylacetonato ligand. The C–N$_{anilido}$ bond at 1.376-(8) Å is shorter than the C–N$_{aniline}$ bonds in **3** (coordinated aniline 1.446(6) Å, 1.425(6) Å and uncoordinated aniline 1.408-(7) Å). The structure of the monocation in **1** is very similar to

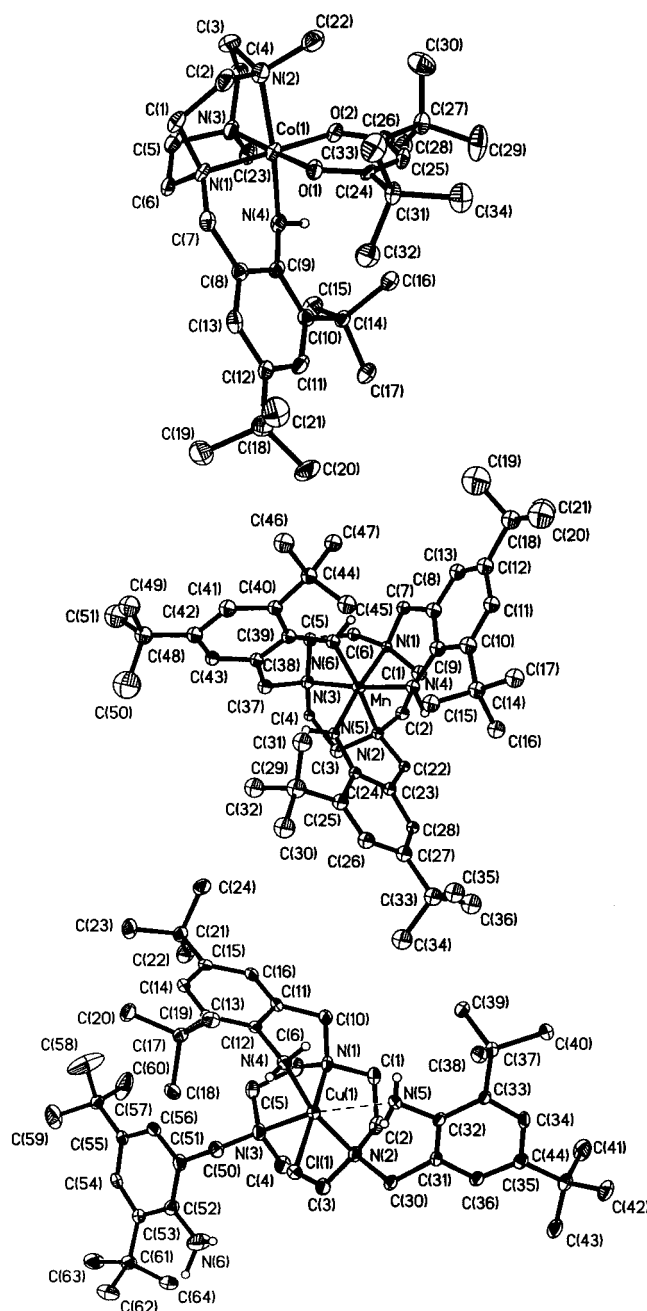**Scheme 3.** Synthesis of Ligands

Figure 1. Structures of the monocations in crystals of **1** (top), **2** (middle), and **3** (bottom). Small open circles represent hydrogen atoms at the aniline nitrogen atoms. All other hydrogens are omitted.

Table 2. Selected Bond Distances (Å) and Angles (deg) of Complexes

Complex 1			
Co1−O1	1.893(4)	Co1−O2	1.895(4)
Co1−N4	1.912(6)	Co1−N1	1.962(5)
Co1−N3	1.989(6)	Co1−N2	2.044(6)
N4−C9	1.376(8)	O1−C24	1.281(7)
O2−C26	1.280(7)	C24−C25	1.394(9)
C25−C26	1.396(9)		
Co1−N4−C9	122.4(4)	N2−Co1−N4	175.1(2)
Complex 2′			
Mn−N1	2.090(7)	Mn−N3	2.058(8)
Mn−N2	2.065(8)	Mn−N4	1.869(8)
Mn−N5	1.875(8)	Mn−N6	1.878(8)
N4−C9	1.395(12)	N5−C24	1.388(11)
N6−C39	1.379(11)		
Mn−N4−C9	126.5(7)	Mn−N5−C24	126.7(6)
Mn−N6−C39	129.5(7)	N6−Mn−N2	170.8(3)
N5−Mn−N1	170.1(3)	N4−Mn−N3	170.7(3)
Complex 3			
Cu−N1	2.065(4)	Cu−N2	2.066(4)
Cu−N3	2.332(4)	Cu−N4	2.038(4)
Cu−N5	2.641(4)	Cu−Cl1	2.305(1)
N4−C12	1.446(6)	N5−C32	1.425(6)
N6−C52	1.408(7)		
Cu−N4−C12	117.9(3)	Cu−N5−C32	123.3(3)

that of the analogous (phenolato)cobalt(III) complex [Co^{III}(L^{Pr})-(acac)](ClO$_4$).[2c]

The manganese(IV) ion of the monocation in crystals of **2′** is in a distorted octahedral environment composed of three facially coordinated amine nitrogen donors of the 1,4,7-triazacyclononane backbone and three anilido nitrogen donor atoms of the three pendant arms of the ligand (L^2)$^{3-}$. The anilido nitrogen atoms are three-coordinate and sp^2-hybridized. The cation possesses idealized C_3 symmetry. The structure of the cation in **2′** is very similar to that reported previously for [Mn^{IV}-(L^a)]BPh4,[14] where (L^a)$^{3-}$ represents the triply deprotonated ligand 1,4,7-tris(*o*-aminobenzyl)-1,4,7-triazacyclononane, which is the unsubstituted analogue of (L^2)$^{3-}$. The average C−N$_{anilido}$ bond distance at 1.387(10) Å is again slightly shorter than the average C−N$_{aniline}$ bond in complexes of divalent metal ions containing the coordinated aniline ligand (H$_3$[L^a]),[15] e.g., in [Ni^{II}-(L^{a}H$_3$)](ClO$_4$)$_2$·H$_2$O at 1.450(10) Å.

Table 3. Electronic Spectra of Complexes in CH_2Cl_2 Solution

complex	λ_{max}, nm (ϵ, L mol^{-1} cm^{-1})
1	$256(2.3 \times 10^4)$, $330sh(4.2 \times 10^3)$, $466(2.2 \times 10^3)$, $672(1.5 \times 10^3)$
$[Co^{III}(L^{1\bullet})(Bu_2acac)]^{2+ \, a}$	$296(2.0 \times 10^4)$, $494(3.0 \times 10^3)$, $592sh(1.8 \times 10^3)$
2	$260(2.9 \times 10^4)$, $296(1.8 \times 10^4)$, $347sh(5.7 \times 10^3)$, $502sh(2.8 \times 10^3)$, $721(1.2 \times 10^4)$
$[Mn^{IV}(L^{2\bullet})]^{2+ \, a}$	$260(2.4 \times 10^4)$, $280(2.1 \times 10^4)$, $355(6.5 \times 10^3)$, $427sh(8.5 \times 10^3)$, $461(9.7 \times 10^3)$, $718(8.9 \times 10^3)$
$[Mn^{IV}(L^{2\bullet\bullet})]^{3+ \, a}$	$270(2.1 \times 10^4)$, $420sh(1.0 \times 10^4)$, $458(1.2 \times 10^4)$, $572(2.0 \times 10^4)$
$[Mn^{IV}(L^{2\bullet\bullet\bullet})]^{4+ \, a}$	$270(2.4 \times 10^4)$, $420sh(1.1 \times 10^4)$, $456(1.5 \times 10^4)$, $543(3.0 \times 10^4)$
3	$276(1.1 \times 10^4)$, $325sh(5.1 \times 10^3)$, $400(3.2 \times 10^3)$, $618(610)$

^{a} Electrochemically generated at -40 °C in CH_2Cl_2 (0.10 M [(n-Bu)$_4$N]PF$_6$).

The monocation in crystals of **3** contains a tetradentate neutral ligand $H_3[L^2]$ where the three amine nitrogen atoms of the 1,4,7-triazacyclononane backbone are bound to the Cu^{II} ion and, in addition, one of the pendant aniline arms. The second aniline arm may be very weakly coordinated to the Cu^{II} ion; this Cu$-$N$_{aniline}$ distance is long at 2.641(4) Å. The third (dangling) pendant arm is definitely not coordinated. Since the Cu^{II} ion is also bound to a Cl$-$ ligand, it possesses a (5 + 1) coordination sphere. The three inequivalent Cu$-$N$_{amine}$ distances at 2.065, 2.066, and 2.332 Å indicate that the former two of these amine nitrogens occupy basal and one the apical position of a square-base pyramidal polyhedron, which is completed by binding to one aniline and a chloride ion the remaining two basal positions. As discussed above, the average C$-$N$_{aniline}$ distances are relatively long in accordance with a C$-$N single bond.

Electro- and Spectroelectrochemistry. Cyclic voltammograms and coulometric experiments of **1**, **2**, and **3** have been measured in CH_2Cl_2 solution containing 0.10 M [(n-Bu)$_4$N]PF$_6$ as supporting electrolyte. Potentials were measured vs the Ag/0.01 M AgNO$_3$/CH$_3$CN reference electrode; ferrocene was used as internal standard. All redox potentials are referenced vs the ferrocenium/ferrocene (Fc$^+$/Fc) couple (0.40 V vs NHE). Table 3 summarizes electronic spectra of electrochemically generated species.

The CV of **1** displays a single reversible one-electron oxidation wave at -0.07 V and an irreversible reduction peak at approximately -1.5 V as well as an irreversible oxidation at $E_p^{ox} = +1.10$ V. The latter two processes have not been further studied.

Figure 2 displays the CV of **1** recorded in the potential range $+0.5$ to -0.6 V. This process corresponds to the formation of the (anilino)cobalt(III) radical $[Co^{III}(L^{1\bullet})(Bu_2acac)]^{2+}$ as was judged from spectral changes observed during the coulometric

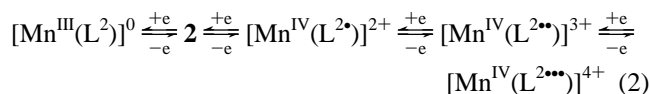$$\mathbf{1} \underset{-e}{\overset{+e}{\rightleftharpoons}} [Co^{III}(L^{1\bullet})(Bu_2acac)]^{2+} \qquad (1)$$
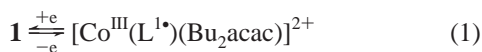
one-electron oxidation of **1** shown in Figure 3. The electronic spectrum of the starting material 1 displays two d$-$d transitions of an octahedral low-spin cobalt(III) ion in the visible at 466 nm ($\epsilon = 2.2 \times 10^3$ L mol^{-1} cm^{-1}) and 672 (1.5×10^3), which, in O_h symmetry, are assigned to $^1A_g \rightarrow {}^1T_{2g}$ and $^1A_{1g} \rightarrow {}^1T_{1g}$ transitions, respectively. Upon one-electron oxidation two new intense absorption maxima are generated at 494 nm ($\epsilon = 3.0 \times 10^3$ L mol^{-1} cm^{-1}) and 592 (1.8×10^3). In addition, a new transition at 296 nm ($\epsilon = 2.0 \times 10^4$ L mol^{-1} cm^{-1}) appears.

Figure 4 shows the CV of **2** in CH_2Cl_2 (0.10 M [(n-Bu)$_4$N]PF$_6$) at different scan rates. Clearly, four reversible one-electron-transfer waves are observed at $E_{1/2} = -1.12$, 0.23, 0.59, and 0.96 V. The first reversible reduction process is probably metal-centered and is assigned to the Mn^{IV}/Mn^{III} couple. The three successive one-electron oxidation processes are ligand-centered
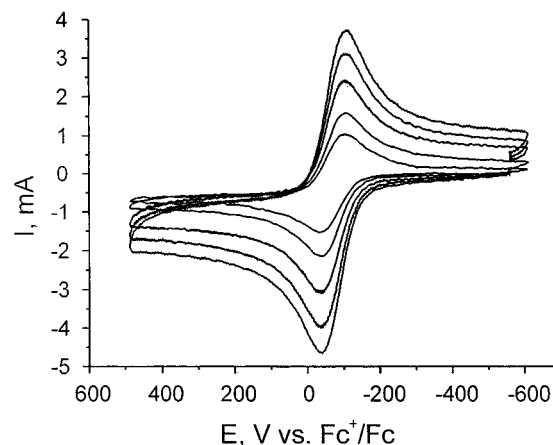
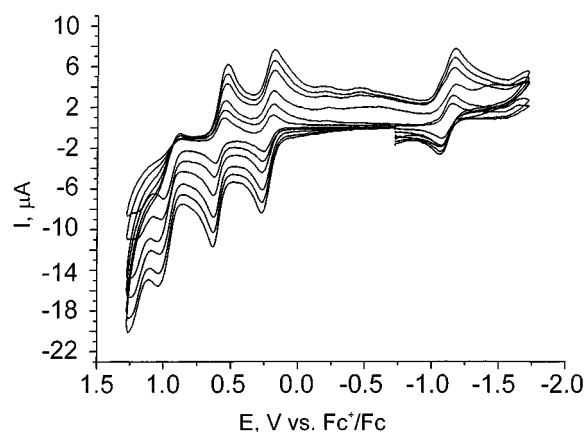**Figure 2.** Cyclic voltammogram of **1** in CH_2Cl_2 (0.10 M [(n-Bu)$_4$N]-PF$_6$) at 298 K (glassy carbon electrode; scan rates: 50, 100, 200, 300, and 400 mV s^{-1}).
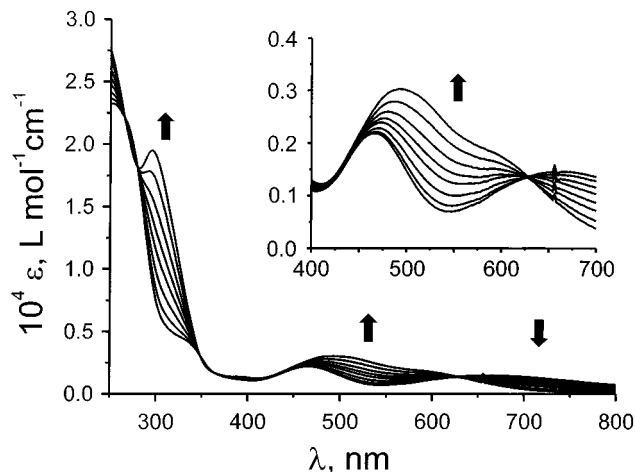
Figure 3. Spectral changes observed during the coulometric oxidation of **1** to $[Co(L^{1\bullet})(Bu_2acac)]^{2+}$ in CH_2Cl_2 (0.10 M [(n-Bu)$_4$N]PF$_6$) at 298 K ([1] = 5×10^{-4} M).

and correspond to the formation of one, two, and three coordinated anilino radicals, eq 2.

$$[Mn^{III}(L^2)]^0 \underset{-e}{\overset{+e}{\rightleftharpoons}} \mathbf{2} \underset{-e}{\overset{+e}{\rightleftharpoons}} [Mn^{IV}(L^{2\bullet})]^{2+} \underset{-e}{\overset{+e}{\rightleftharpoons}} [Mn^{IV}(L^{2\bullet\bullet})]^{3+} \underset{-e}{\overset{+e}{\rightleftharpoons}} [Mn^{IV}(L^{2\bullet\bullet\bullet})]^{4+} \quad (2)$$

Coulometric measurements at appropriately fixed potentials in CH_2Cl_2 solution at -40 °C showed that all three oxidations of **2** are reversible on the time scale of these experiments ($\sim$20 min). At room temperature this is not the case; they are irreversible. It has been possible to characterize these oxidized species by UV/vis and EPR spectroscopy at -40 °C.

Figure 5 shows the spectral changes observed during the oxidation of **2** to $[Mn^{IV}(L^{2\bullet})]^{2+}$ (top), $[Mn^{IV}(L^{2\bullet})]^{2+}$ to $[Mn^{IV}(L^{2\bullet\bullet})]^{3+}$ (middle), and, finally, to $[Mn^{IV}(L^{2\bullet\bullet\bullet})]^{4+}$ (bottom).

Figure 4. Cyclic voltammogram of **2** in CH$_2$Cl$_2$ (0.10 M [(n-Bu)$_4$N]-PF$_6$) at 298 K (glassy carbon electrode; scan rates: 50, 100, 200, 300, 400, and 500 mV s^{-1}).
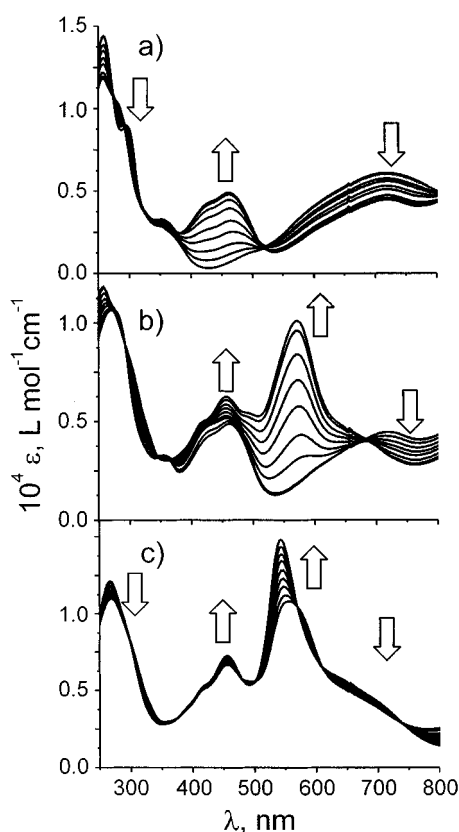

Figure 5. Spectral changes observed during the coulometric oxidation of (a) **2** to [Mn^{IV}(L$^{2\bullet}$)]$^{2+}$, (b) [Mn^{IV}(L$^{2\bullet}$)]$^{2+}$ to [Mn^{IV}(L$^{2\bullet\bullet}$)]$^{3+}$, and (c) [Mn^{IV}(L$^{2\bullet\bullet}$)]$^{3+}$ to [Mn^{IV}(L$^{2\bullet\bullet\bullet}$)]$^{4+}$ in CH$_2$Cl$_2$ (0.10 M [(n-Bu)$_4$N]PF$_6$) at 233 K.

The electronic spectrum of the starting material **2** displays a very intense anilido-to-manganese(IV) charge-transfer (CT) band at 721 nm and a shoulder at 502 nm. Note that an absorption minimum is observed at ∼420 nm. Upon one-electron oxidation the intensity of the CT band at 721 nm decreases whereas two new intense maxima appear at 427sh (8.5 × 10^3 L mol^{-1} cm^{-1}) and 461 nm (9.7 × 10^3 L mol^{-1} cm^{-1}), which are assigned to π−π* transitions of the coordinated anilino radical. These absorptions are observed as broad maximum at 400 nm (ε = 1.3 × 10^3) for the uncoordinated anilino radical, Ph−ṄH, and for the anilino radical cation [Ph−ṄH$_2$]$^+$ at 423 (4.1 × 10^3) and 406 nm (3.3 × 10^3 L mol^{-1} cm^{-1}) according to Tripathi and Schuler.[6a] Thus coordination of an anilino radical to a Mn^{IV}

ion induces a bathochromic shift of these π−π* bands and an increase in intensity.

Upon further one-electron oxidation to [Mn^{IV}(L$^{2\bullet\bullet}$)]$^{3+}$ the spectrum changes again significantly. The intensity of the π−π* anilino radical transitions at 420 and 458 nm increases, and, in addition, a very intense new absorption maximum at 572 nm (ε = 2.0 × 10^4 L mol^{-1} cm^{-1}) is observed. Further oxidation to [Mn^{IV}(L$^{2\bullet\bullet\bullet}$)]$^{4+}$ slightly increases the intensity of the anilino π−π* transitions and dramatically enhances the latter band, which at the same time is hypsochromically shifted to 543 nm (ε = 3.0 × 10^4). The latter band is very similar to those observed in tris(semiquinonato)chromium(III) and tris(phenoxyl)chromium(III) complexes.[22] Güdel and Dei et al.[23] have assigned this transition to a spin-forbidden transition $^4A_{2g} \rightarrow {}^2E_g$ (in O_h symmetry) corresponding to a spin-flip in the ground state. This transition is believed to gain intensity by 3 orders of magnitude by strong exchange coupling between the Cr^{III} ion and the O-coordinated radicals. We propose a similar mechanism for the band at 572 nm in [Mn^{IV}(L$^{2\bullet\bullet}$)]$^{3+}$ and at 543 nm in [Mn^{IV}-(L$^{2\bullet\bullet\bullet}$)]$^{4+}$. Thus the electronic spectra of the three oxidized forms of **2** clearly show that one, two, and three coordinated anilino radicals are successively formed.

Complex **3** contains one N-coordinated aniline pendent arm, a dangling uncoordinated aniline arm, and a very weakly N-bound aniline arm. The CV of **3** displays at ambient temperature a quasi-reversible one-electron oxidation wave at $E_{1/2}$ = 0.66 V and an irreversible reduction at −1.08 V. One-electron oxidation of **3** produces the aniline radical cation, which may be coordinated to the Cu^{II} ion or not. The oxidized form is not stable on the time scale of a coulometric measurement, and, therefore, it has not been possible to characterize this species spectroscopically.

X-Band EPR Spectroscopy. The X-band EPR spectrum at 295 K of electrochemically generated [Co^{III}(L$^{1\bullet}$)(Bu$_2$acac)]$^{2+}$ in CH$_2$Cl$_2$ solution (0.10 M [(n-Bu)$_4$N]PF$_6$) shown in Figure 6 displays a signal centered at g = 2.0023 with well-resolved hyperfine structure indicating the presence of a coordinated anilino radical. The experimental spectrum has been successfully simulated by using the parameters indicated in Figure 6. Strong hyperfine coupling to a ^{59}Co nucleus (I = 7/2) in conjunction with coupling to a proton of the diastereotopic benzyl group (a(^{59}Co) = 1.215 mT; a(^{1}H) = 0.856 mT) prove that the anilino radical is coordinated. The hyperfine coupling to the anilino nitrogen and an (NH) proton prove that the anilide in **1** is one-electron oxidized. The spectrum of the deuterated radical complex [Co(d$_4$-L$^{1\bullet}$)(Bu$_2$acac)]$^{2+}$ and its simulation are also shown in Figure 6. The spectrum has been simulated using the same set of parameters as above for the [Co^{III}(L$^{1\bullet}$)(Bu$_2$acac)]$^{2+}$ species with the exception of one benzylic deuteron for which a coupling constant of a(^{2}H) = 0.141 mT was found. The ratio a(^{1}H)/a(^{2}H) of 6.52 is in accord with this interpretation.

By using a McConnell-type relationship for the hyperfine coupling to the benzylic protons where the magnitude of a(^{1}H) depends on cos^2 θ_1 and cos^2 θ_2 as defined in Scheme 4, we calculated an a(^{1}H) value for the second benzylic proton of 0.38 mT. The dihedral angles θ_1 and θ_2 were taken from the crystal structure of **1** and are assumed to be the same in its oxidized form. This coupling is clearly seen in the experimental spectrum

(22) (a) Buchanan, R. M.; Kessel, S. L.; Downs, H. H.; Pierpont, C. G.; Hendrickson, D. N. *J. Am. Chem. Soc.* **1978**, *100*, 7894. (b) Sofen, S. R.; Ware, D. C.; Cooper, S. R.; Raymond, K. N. *Inorg. Chem.* **1979**, *18*, 234. (c) Downs, H. H.; Buchanan, R. M.; Pierpont, C. G. *Inorg. Chem.* **1979**, *18*, 1736. (d) Buchanan, R. M.; Clafin, J.; Pierpont, C. G. *Inorg. Chem.* **1983**, *22*, 2552.
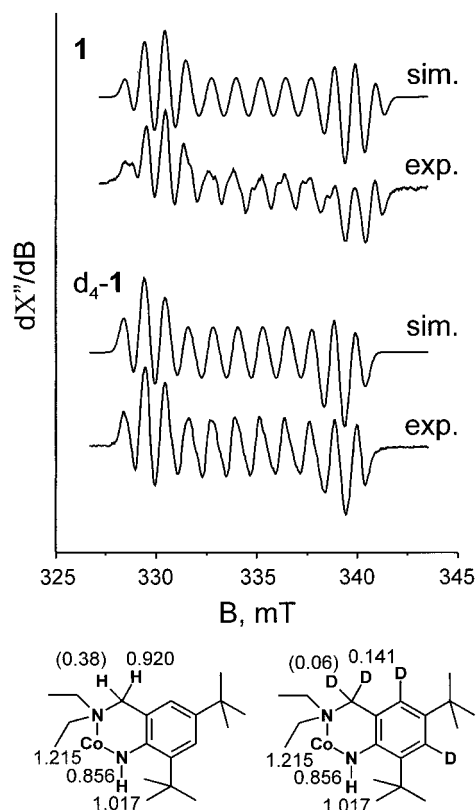(23) Benelli, C.; Dei, A.; Gatteschi, D.; Güdel, H. U.; Pardi, L. *Inorg. Chem.* **1989**, *28*, 3089.

Figure 6. X-band EPR spectra of electrochemically one-electron oxidized **1** and d$_4$-**1** at 298 K in CH$_2$Cl$_2$ (0.10 M [(*n*-Bu)$_4$N]PF$_6$) solution and their simulations using hyperfine coupling constants in units of [mT] as depicted in the formulas (at $g = 2$ a hyperfine splitting of 1 mT corresponds to a coupling constant of $a = 9.35 \times 10^{-4}$ cm^{-1}). Conditions: frequency, 9.4420 GHz for **1** and 9.4597 GHz for d$_4$-**1**; modulation, 0.02 mT; power, 1.0 mW for **1** and 10 mW for d$_4$-**1**. Simulation parameters: Gaussian lines with $W_{iso} = 0.104$ mT for **1** and 0.109 mT for d$_4$-**1**.

Scheme 4. Definition of Dihedral Angles θ_1, θ_2 at the Benzyl Group of **1**
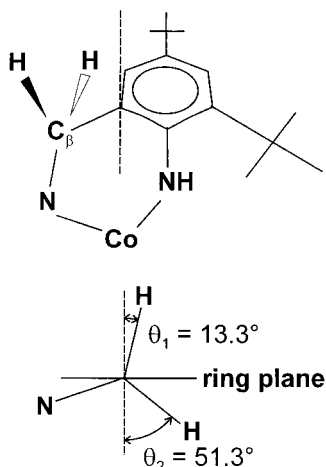
as asymmetric shoulders. It has not been possible to include this coupling satisfactorily in the simulations, but note that for [Co^{III}(d$_4$-L$^{1\bullet}$)(Bu$_2$acac)]$^{2+}$ this coupling constant is only 0.06 mT and, consequently, it is not observed in the spectrum. Hyperfine couplings to the aromatic protons in meta position to the NH group are not resolved; they are expected to be small.

It is instructive to compare these data with those reported for the 2,4,6-tri-*tert*-butylanilino radical[7b,c] ($a(^{14}N) = 0.67$ mT and $a(^1H, \dot{N}H) = 1.19$ mT) and the unsubstituted anilino
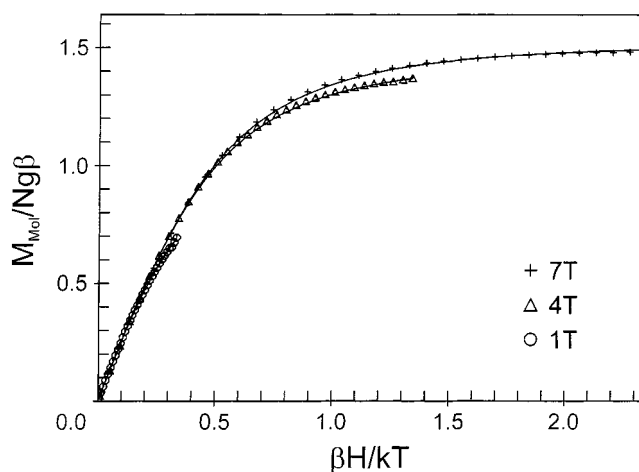
Figure 7. Temperature-dependent magnetization measurements of **2′** at magnetic fields of 1, 4, and 7 T. Solid lines represent a best fit using parameters given in the text.

radical[7a] ($a(^{14}N) = 0.80$ mT, $a(^1H, NH) = 1.29$ mT). In all cases the large values for $a(^{14}N)$ and the $a(^1H, NH)$ hyperfine coupling constants indicate a significant spin density at the anilino nitrogen. It is interesting that the $a(^{59}Co)$ hyperfine coupling constant of [Co^{III}(L$^{Pr\bullet}$)(acac)]$^{2+}$ at 0.6 mT[2e] is significantly smaller indicating that the Co—N$_{anilino}$ bond is stronger and more covalent than the corresponding Co—O$_{phenoxyl}$ bond.

The electronic structure of solid, magnetically dilute **2′** has been characterized by field- and temperature-dependent magnetization measurements shown in Figure 7 by using a SQUID magnetometer. The compound possesses the expected $S = 3/2$ ground state for an octahedral Mn^{IV} ion (d^3). From simulations an isotropic g value of 2.03, and axial and rhombic zero-field splitting (ZFS) parameters $|D| = 1.26$ cm^{-1} and $E/D = 0.06$ have been determined. Thus, the system is in the limit of strong ZFS with respect to X-band EPR ($2D \gg h\cdot\nu \sim 0.3$ cm^{-1}). The Zeeman splitting is smaller than ZFS in the whole field range of X-band spectra, and only the transitions within the $m_s = \pm 1/2$ doublet are observable. For axial symmetry ($E/D = 0$) signals would be expected at effective g values of $g_\perp \sim 4$ and $g_{||} \sim 2$. Indeed, the X-band EPR spectrum of **2′** at 5 K shown in Figure 8 displays an axial signal with well-resolved ^{55}Mn hyperfine splitting at $g_{||}$. The spectrum was readily simulated using D, E/D values from the magnetization measurements with $g_{iso} = 2.000$ and $a(^{55}Mn) = 70 \times 10^{-4}$ cm^{-1} (7.5 mT).

The X-band EPR spectrum of the electrochemically generated complex [Mn^{IV}(L$^{2\bullet}$)]$^{2+}$ in CH$_2$Cl$_2$ solution at 10 K is shown in Figure 9. The signal around $g = 2.0$ is most probably due to a small amount (<4%) of overoxidized [Mn^{IV}(L$^{2\bullet\bullet}$)]$^{3+}$ (see Figure 11). At higher power weak signals at $g = 4-7$ are observed indicating that the monoradical is an integer spin system ($S_t = 1$ or $S_t = 2$). These signals display a different saturation behavior than the signal at $g = 2$, indicating that the signals belong to different species. We have simulated the weak signal assuming an $S_t = 1$ system. The ZFS parameter $D_t \sim 2.0$ cm^{-1} and $E = 0.14$ cm^{-1} at $g_{iso} = 2.000$ were obtained, if a small impurity ($\ll 1$%) of the starting material **2** is assumed to be present. It is not unequivocally possible to discern an $S_t = 1$ from an $S_t = 2$ ground state for [Mn^{IV}(L$^{2\bullet}$)]$^{2+}$ on the basis of this EPR spectrum alone as shown in Figure 10, but in light of the observed strong antiferromagnetic coupling in [Cr^{III}(L$^{\bullet}$)]$^{+}$ [24] a (phenoxyl)chromium(III) species we favor an $S_t = 1$ ground

(24) Sokolowski, A.; Bothe, E.; Bill, E.; Weyhermüller, T.; Wieghardt, K. *Chem. Commun.* **1996**, 1671.
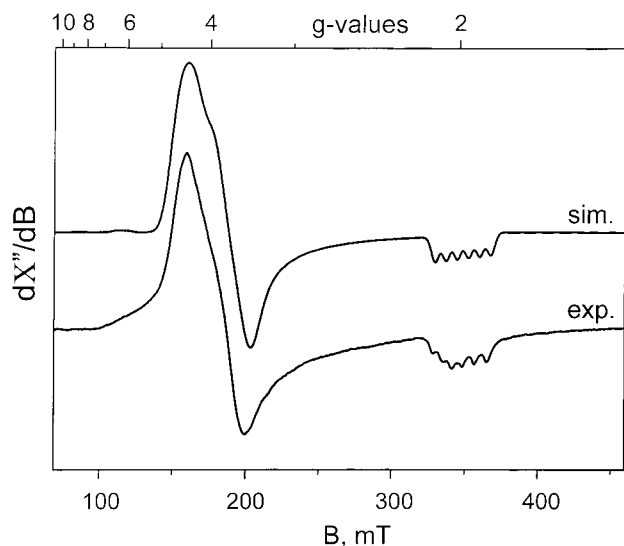
Figure 8. X-band EPR spectrum of **2** in CH_2Cl_2 at 5 K. Conditions: frequency, 9.6446 GHz; modulation, 1.28 mT; power, 1.6 mW. Simulation parameters are given in the text (Gaussian lines with angular-dependent line widths $W = -\{14, 14, 5\}$ mT).
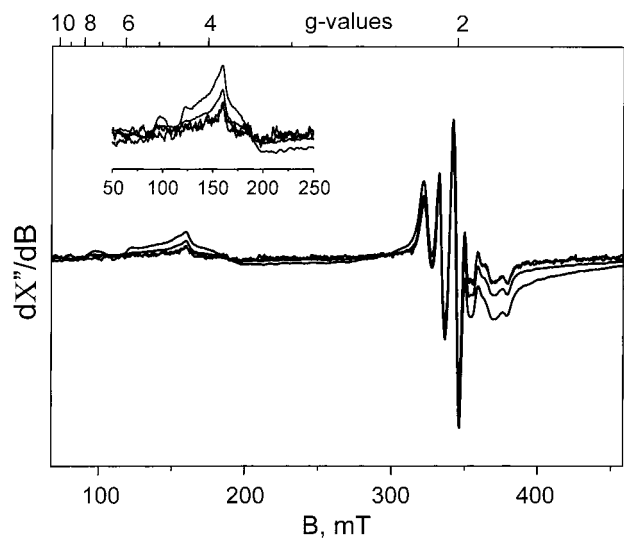

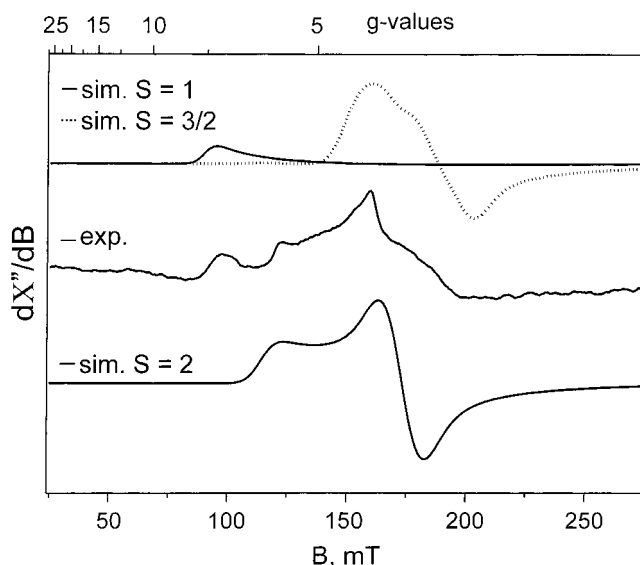**Figure 10.** Experimental EPR spectrum (10 K) and two simulations for $S = 1$ and $S = 2$ of $[Mn^{IV}(L^{2\bullet})]^{2+}$. Frequency-constant line widths of $W_f = 70$ mT at $g = 2$ and $W_f = 60$ mT at $g = 2$ were used for the simulations with $S = 1$ and $S = 2$, respectively. Experimental conditions: frequency, 9.4630 GHz; modulation, 1.28 mT; power, 50.4 mW. The dotted line in the top spectrum shows a simulated contribution from unoxidized starting material $[Mn^{IV}(L^2)]^+$ ($S = 3/2$) as shown in Figure 8, which amounts to ∼2% of the nonoxidized sample.

Figure 9. X-band EPR spectra of electrochemically generated $[Mn^{IV}\text{-}(L^{2\bullet})]^{2+}$ in CH_2Cl_2 at 10 K recorded at power 100.6 μW, 504.1 μW, 5.0 mW, and 50.4 mW. Conditions: frequency, 9.4630 GHz; modulation, 1.28 mT. The inset shows the integer-spin signal at $g \sim 4$ with increasing power.

state, which is attained via antiferromagnetic coupling between a Mn^{IV} ion (d^3, $S_{Mn} = 3/2$) and an anilino radical ($S_{Rad} = 1/2$).

The X-band EPR spectrum of the electrochemically generated diradical $[Mn^{IV}(L^{2\bullet\bullet})]^{3+}$ in CH_2Cl_2 solution at 10 K is shown in Figure 11 along with its simulation. A typical $S = 1/2$ signal at $g = 1.965$ with resolved ^{55}Mn hyperfine coupling is observed ($a(^{55}Mn) = 70 \times 10^{-4}$ cm^{-1}; 7.5 mT).

Assuming intramolecular antiferromagnetic coupling between the Mn^{IV} ions and the anilino radicals to prevail, we expect the triradical $[Mn^{IV}(L^{2\bullet\bullet\bullet})]^{4+}$ to possess a singlet ground state ($S_t = 0$). Indeed, upon one-electron oxidation of $[Mn^{IV}(L^{2\bullet\bullet})]^{3+}$ its $S = 1/2$ signal gradually disappears. The triradical is EPR silent.

Resonance Raman Spectroscopy. To gain further information on characteristic spectroscopic features of coordinated anilino radicals we have measured RR spectra of electrochemically generated $[Co^{III}(L^{1\bullet})(Bu_2acac)]^{2+}$ and its deuterated analogue $[Co(d_4\text{-}L^{1\bullet})(Bu_2acac)]^{2+}$ in CH_2Cl_2 solutions containing 0.1 M $[(n\text{-}Bu)_4N]PF_6$. The spectra were recorded at 20 °C by
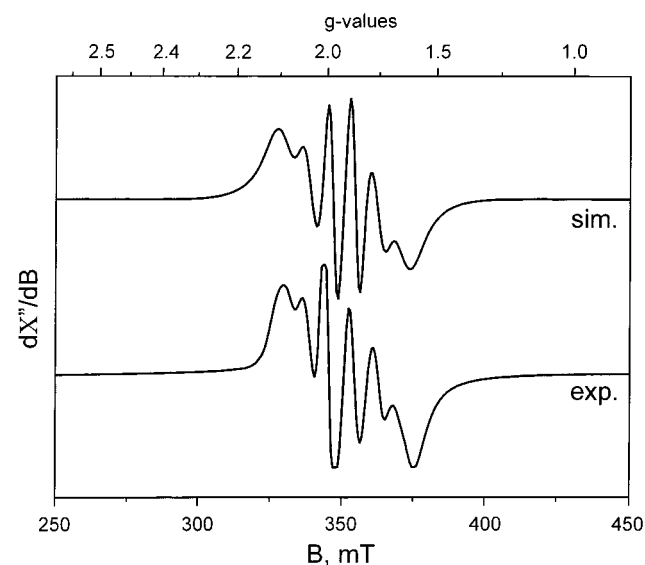

Figure 11. X-band EPR spectrum of electrochemically generated $[Mn^{IV}(L^{2\bullet\bullet})]^{3+}$ in CH_2Cl_2 (0.10 M $[(n\text{-}Bu)_4N]PF_6$) at 10 K and simulation. Conditions: frequency, 9.6447 GHz; modulation, 1.28 mT; power, 1.6 mW. Simulation parameters are given in the text. The line widths for the simulated spectrum are determined according to $\sigma(field) = (\Sigma_{i=x,y,z}\sigma_i^2 l_i^2)^{1/2}$, where l_i denotes the direction cosines and σ_i the angular dependent line width. Here, $\sigma_i^2 = W_i + C_{1,i}\cdot\nu + \Sigma m_l C_{2,i}\cdot m_l^2$, where W_i is the intrinsic residual line width, ν is the microwave frequency, and $m_l = -5/2\cdots+5/2$ is the magnetic quantum number of the ^{55}Mn nucleus ($l = 5/2$). For further details, see, for instance: Pilbrow, J. R. *Transition Ion Electron Paramagnetic Resonance*; Clarendon Press: Oxford, 1990. The line shape parameters used are $W = \{0, 3.5, 3.5\}$ mT, $C_{1x} = 4$ mT/GHz, $C_{2y} = 2$ mT, $C_{2z} = 2$ mT.

using the excitation line 514 nm coincident with the anilino radical $\pi \rightarrow \pi^*$ transitions. Under the same conditions, no Raman bands could be detected for the parent compounds **1** and d$_4$-**1** so that the RR bands in the spectra shown in Figure 12 exclusively originate from the radical complexes.
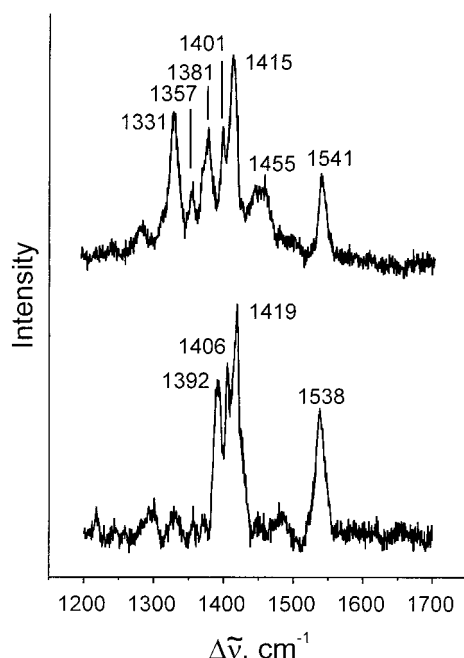
Figure 12. Resonance Raman spectra of electrochemically generated $[Co^{III}(L^{1\bullet})(Bu_2acac)]^{2+}$ (top) and $[Co^{III}(d_4\text{-}L^{1\bullet})(Bu_2acac)]^{2+}$ (bottom) in CH_2Cl_2 (0.10 M $[(n\text{-}Bu)_4N]PF_6$) measured at 298 K with 514 nm excitation.

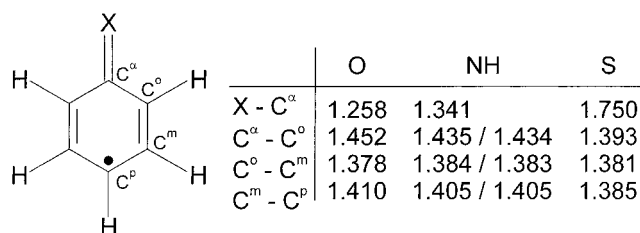|	O	NH	S
X - C^α	1.258	1.341	1.750
C^α - C^o	1.452	1.435 / 1.434	1.393
C^o - C^m	1.378	1.384 / 1.383	1.381
C^m - C^p	1.410	1.405 / 1.405	1.385

Figure 13. Calculated structures of phenoxyl, anilino, and phenylthiyl radicals from refs 9 and 25. Bond distances are given in Å.

deuterated complex indicating that the underlying modes include much smaller contributions of the C−H in-plane bending coordinates.

Discussion

The structures of the uncoordinated phenoxyl,[9] anilino,[9] and phenylthiyl[25] free radicals have been established by hybrid Hartree/Fock density functional calculations. The results are summarized in Figure 13. It appears that the phenoxyl and anilino radicals both have a quinoid type structure with two relatively short C^o=C^m bonds between the carbon atoms in ortho and para positions relative to the C=X (X = O, NH) bond. In contrast, all the C−C bonds of the phenylthiyl radical are nearly equidistant. The calculated spin densities and EPR spectroscopic measurements are in excellent agreement with the interpretation that in the phenoxyl and anilino radical the unpaired electron is delocalized but localized in the phenylthiyl. Thus, the latter is best described as an S-centered radical. Furthermore, the C=O and C=N bonds in the phenoxyl and anilino radicals are considerably shorter than in their diamagnetic one-electron reduced anions, namely, the phenolate and anilide. These features are in general retained in O-coordinated phenoxyl radicals as has been verified experimentally by comparison of the structures of $[Cr^{III}L]\cdot2CH_3CN$ and its one-electron oxidized form $[Cr^{III}L\bullet](ClO_4)\cdot3CH_3CN$, the latter of which contains two phenolato and a clearly discernible phenoxyl pendent arm.[24] The ligand L is 1,4,7-tris(3-*tert*-butyl-5-methoxy-2-hydroxybenzyl)-1,4,7-triazacyclononane, H_3L. Therefore, one can expect that the electronic structures of an anilino and of a phenoxyl radical each coordinated to a transition metal ion and their spectroscopic properties are in fact quite similar.

This is indeed the case as is shown by comparison of the phenoxyl radical complex $[(L^{Pr\bullet})Co^{III}(acac)]^{2+}$[2e] and its anilino radical analogue $[(L^{1\bullet})Co^{III}(Bu_2acac)]^{2+}$. Both paramagnetic species have an $S = 1/2$ ground state and display very informative X-band EPR spectra at 295 K with a well-resolved hyperfine splitting pattern. It is important to reemphasize that the hyperfine coupling constant of the anilino nitrogen $a(^{14}N) = 0.856$ mT is nearly the same in the unsubstituted, free anilino radical[7a] at $a(^{14}N) = 0.80$ mT and 0.67 mT in the 2,4,6-tri-*tert*-butylanilino radical.[7b,c]

The electronic spectrum of $[Co^{III}(L^{1\bullet})(Bu_2acac)]^{2+}$ displays intense absorption maxima ($>10^3$ L mol^{-1} cm^{-1}) at 494 and 592 nm, which are absent in the one-electron reduced starting material 1. These absorptions resemble closely the $\pi \rightarrow \pi^*$ transitions of the anilino radical cation at 406 and 423 nm.[6a] This assignment is bolstered by the fact that upon excitation in resonance with one of these $\pi \rightarrow \pi^*$ transitions of the coordinated anilino radical in $[Co^{III}(L^{1\bullet})(Bu_2acac)]^{2+}$ the RR modes originating from the anilino radical are detectable. Very similar observations have been reported for the phenoxyl radical

Quantum chemical calculations have predicted similar normal-mode patterns for anilino and phenoxyl radicals.[9] For both radicals, excitation in resonance with the $\pi \rightarrow \pi^*$ transition provides enhancement of the totally symmetric modes leading to up to four prominent bands in the spectral region between 1200 and 1700 cm^{-1}.[3,8] As documented by various examples, the principle features of these RR spectra are largely independent of the substitution pattern of the radical.[2b−e,3] Consequently, the highest-frequency band in the RR spectrum of $[Co(L^{1\bullet})(Bu_2acac)]^{2+}$ at 1541 cm^{-1} is readily assigned to the stretching of the C_{ortho}−C_{meta} bonds, reflecting the quinoid structure of the anilino radical. This band reveals only a small downshift in the deuterated radical complex, which supports the assignment to an essentially pure C−C stretching mode, denoted as ν_{8a} for the sake of simplicity.[3] The distinctly lower frequency of this mode compared to that of free unsubstituted anilino radicals[8,9] may result from the *tert*-butyl substituents in ortho and para position. A plausible candidate for the mode that involves the C−NH stretching is the band at 1331 cm^{-1} as its frequency agrees well with the calculated value.[9] This band disappears in the RR spectrum of the deuterated radical complex. This unique sensitivity toward ring deuteration can be understood on the basis of the composition of the corresponding mode in phenoxyl radicals, denoted as ν_{7a}, for which a substantial coupling of the C−O stretching and the C−H in-plane bending coordinates was found.[3] It is very likely that an analogous composition holds for ν_{7a} of anilino radicals in view of the overall similarity in the character of the modes with phenoxyl radicals.[9] Upon ring deuteration, this coupling is removed so that the compositions of ν_{7a} and the adjacent modes are drastically altered leading to pronounced changes in the spectrum between 1300 and 1400 cm^{-1}. Specifically, the three bands at 1331, 1357, and 1381 cm^{-1} of $[Co(L^{1\bullet})(Bu_2acac)]^{2+}$ are replaced by a single band at 1392 cm^{-1} in $[Co(d_4\text{-}L^{1\bullet})(Bu_2acac)]^{2+}$, which most likely originates from a mode of predominant C−NH stretching character. The remaining bands at 1401 and 1415 cm^{-1} of $[Co(L^{1\bullet})(Bu_2acac)]^{2+}$ reveal only slight frequency upshifts in the

(25) Tripathi, G. N. R.; Sun, Q.; Armstrong, D. A.; Chipman, D. N.; Schuler, R. H. *J. Phys. Chem.* **1992**, *96*, 5345.

species $[Co^{III}(L^{Pr•})(acac)]^{2+}$.[2e] Thus, for both Co^{III} complexes the RR spectra indicate a quinoid structure of the coordinated ligand radical.

The redox potentials for the couples $Ph-\overset{•}{N}H/Ph-NH^-$ and $Ph-\overset{•}{N}H_2^+/Ph-NH_2$ have been determined by pulse radiolysis and electrochemical methods to be -0.99 V vs Fc^+/Fc (in dimethyl sulfoxide) and $+0.445$ V, respectively.[26] For comparison, the redox potential for the couple $Ph-\overset{•}{O}/Ph-O^-$ is ~ 0.4 V vs Fc^+/Fc.[27] Thus a phenolate is relatively difficult to oxidize, but the isoelectronic anilide is a strong one-electron reductant. Interestingly, the redox potentials for the couples $Ph-\overset{•}{O}/Ph-O^-$ and $Ph-\overset{•}{N}H_2^+/Ph-NH_2$ are similar.

From cyclic voltammetry it has been shown that the redox potentials of the couples $[Co^{III}(L^{Pr})(acac)]^{2+/1+}$ at 0.46 V vs Fc^+/Fc[2e] and $[Co^{III}(L^1)(Bu_2acac)]^{2+/1+}$ at -0.07 V differ by 0.53 V. This amounts to less than one-half of the difference between the couples $Ph-\overset{•}{O}/Ph-O^-$ and $Ph-\overset{•}{N}H/Ph-NH^-$ ($\Delta E \sim 1.4$ V). We take this as an indication that the $Co^{III}-N$ bonds of the coordinated anilide in **1** and/or its one-electron oxidized form are more covalent than the $Co^{III}-O$ bonds in the $Co^{III}-$phenolate and/or $Co^{III}-$phenoxyl species. Spectroscopically, this conclusion is bolstered by the hyperfine coupling constants $a(^{59}Co)$ observed for the radical species $[Co^{III}(L^{Pr•})(acac)]^{2+}$ at 0.60 mT[2e] and at 1.215 mT for the analogous $[Co^{III}(L^{1•})(Bu_2acac)]^{2+}$ species.

Interestingly, $[Mn^{IV}(L^{Bu})]^+$, which is the phenolate analogue of **2**, does not exhibit a ligand-centered oxidation up to $+0.7$ V vs Fc^+/Fc. By using the above potential difference of 0.53 V for the structurally analogous phenolate/anilido cobalt com-

plexes, one can calculate the redox potential for the couple $[Mn^{IV}(L^{Bu})]^{2+/+}$ to be $0.23 + 0.53 = 0.76$ V. $H_3[L^{Bu}]$ represents the ligand 1,4,7-tris(3,5-di-*tert*-butyl-2-hydroxybenzyl)-1,4,7-triazacyclononane.[2a] Replacing the *tert*-butyl group in the para position relative to the phenol oxygen by a methoxy group gives the ligand $H_3[L^{OCH3}]$, 1,4,7-tris(3-*tert*-butyl-5-methoxy-2-hydroxybenzyl)-1,4,7-triazacyclononane. This substitution in the para position lowers the redox potential for the phenoxyl/phenolate couple by ~ 250 mV as compared to its unsubstituted parent molecule.[27] Accordingly, for $[Mn^{IV}(L^{OCH3})]^+$ a reversible, ligand-centered one-electron oxidation has been observed at 0.56 V vs Fc^+/Fc.[2a]

The electronic structures of the anilino radical species $[Mn^{IV}(L^{2•})]^{2+}$, $[Mn^{IV}(L^{2••})]^{3+}$, and $[Mn^{IV}(L^{3•••})]^{4+}$ are governed by a strong intramolecular antiferromagnetic coupling between the t_{2g}^3 electronic configuration of the central manganese(IV) ion and one, two, and three anilino radicals ($S_{rad} = 1/2$). Thus electronic ground states of $S = 1$, $1/2$, and 0 are observed for the di-, tri-, and tetracation, respectively. This is also in excellent agreement with the corresponding chromium(III) cations $[Cr^{III}(L^{OCH3•})]^{1+}$, $[Cr^{III}(L^{OCH3••})]^{2+}$ and $[Cr^{III}(L^{OCH3•••})]^{3+}$, which have an $S = 1$, $1/2$, and 0 ground state, respectively.[24]

Supporting Information Available: Tables of crystallographic and structure refinement data, atom coordinates, bond lengths and angles, anisotropic thermal parameters, and calculated positional parameters of H atoms for complexes **1**, **2′·toluene**, and **3·MeOH·1.5H₂O** (PDF). An X-ray crystallographic file, in CIF format, is also available. This material is available free of charge via the Internet at http://pubs.acs.org.

JA001637L

(26) (a) Jansson, M.; Lind, J.; Eriksen, T. E.; Merényi, G. *J. Chem. Soc., Perkin Trans. 2* **1993**, 1567. (b) Lind, J.; Shen, X.; Eriksen, T. E.; Merényi, G. *J. Am. Chem. Soc.* **1990**, *112*, 479. (c) Jonsson, M.; Wayner, D. D. M.; Lusztyk, J. *J. Phys. Chem.* **1996**, *100*, 17539. (d) Jonsson, M.; Lind, J.; Merényi, G.; Eriksen, T. E. *J. Chem. Soc., Perkin Trans. 2* **1995**, 61. (e) Jonsson, M.; Lind, J.; Eriksen, T. E.; Merényi, G. *J. Am. Chem. Soc.* **1994**, *116*, 1423. (f) Bordwell, F. G.; Zhang, X.-M.; Cheng, J.-P. *J. Org. Chem.* **1993**, *58*, 6410. (g) Bordwell, F. G.; Cheng, J.-P. *J. Am. Chem. Soc.* **1991**, *113*, 1736.
(27) (a) Harriman, A. *J. Phys. Chem.* **1987**, *91*, 6102. (b) Surdhar, P. S.; Armstrong, D. A. *J. Phys. Chem.* **1987**, *91*, 6532. (c) Merényi, G.; Lind, J.; Shen, X. *J. Phys. Chem.* **1988**, *92*, 134.